

A Theoretical Framework for Discovering Groups and Unitary Representations via Tensor Factorization

Dongsung Huh

IBM Research

DONGSUNGHUH@GMAIL.COM

Halyun Jeong

University at Albany, State University of New York

HJEONG2@ALBANY.EDU

Abstract

We analyze the HyperCube model, an *operator-valued* tensor factorization architecture that discovers group structures and their unitary representations. We provide a rigorous theoretical explanation for this inductive bias by decomposing its objective into a term regulating factor scales (\mathcal{B}) and a term enforcing directional alignment ($\mathcal{R} \geq 0$). This decomposition isolates the *collinear manifold* ($\mathcal{R} = 0$), to which numerical optimization consistently converges for group isotopes. We prove that this manifold admits feasible solutions exclusively for group isotopes, and that within it, \mathcal{B} exerts a variational pressure toward unitarity. To bridge the gap to the global landscape, we formulate a *Collinearity Dominance Conjecture*, supported by empirical observations. Conditional on this dominance, we prove two key results: (1) the global minimum is achieved by the unitary regular representation for groups, and (2) non-group operations incur a strictly higher objective value, formally quantifying the model’s inductive bias toward the associative structure of groups (up to isotopy).

Keywords: Symmetry Groups, Group Discovery, Unitarity Bias, Tensor Factorization

1. Introduction

Identifying latent algebraic structure—especially group structure—is a cornerstone of scientific discovery. Groups formalize the notion of symmetry, the fundamental principle that generalizes local observations into universal laws of nature (Noether, 1918). Indeed, the discovery of symmetry groups has been essential to the development of modern physics (Wigner, 1967; Gross, 1996).

In deep learning, this principle is operationalized through *Equivariant Neural Networks*, which constrain models to respect specific, a priori known symmetries (Bronstein et al., 2021). While this hard-coded structure leads to superior generalization and sample efficiency (Cohen and Welling, 2016), it limits the model’s applicability if the assumed symmetry is too restrictive or mismatched to the data. Consequently, the recent trend has shifted toward highly flexible, unstructured architectures (e.g., Transformers) that impose minimal symmetry assumptions (Vaswani et al., 2017). While these models can capture complex patterns given vast amounts of data and compute, their lack of structural inductive bias exposes them to fundamental limitations, including low sample efficiency, susceptibility to *shortcut learning* (Geirhos et al., 2020) and *hallucinations* (Ji et al., 2023), and a failure to generalize systematically out-of-domain (OOD) (Lake and Baroni, 2018).

The central open challenge, therefore, is to achieve the best of both worlds: to impose a high-level inductive bias that allows flexible models to **discover** symmetry groups directly

from data, rather than assuming them from the start. However, automating this discovery remains a significant technical hurdle. The discrete axioms of group theory—particularly associativity—are inherently non-differentiable and incompatible with standard gradient-based optimization. As a result, symmetry discovery remains largely a manual endeavor, contingent upon prior expert domain knowledge.

The *HyperCube* model (Huh, 2025) offers a differentiable relaxation of this problem by modeling algebraic operations via an **operator-valued tensor factorization** equipped with a native regularization objective. Empirically, HyperCube demonstrates a strong inductive bias toward discovering groups and their unitary representations from observed data. However, a theoretical explanation for this bias has remained elusive.

Goal. Our primary objective is to theoretically characterize HyperCube’s optimization landscape to explain the mechanism behind two distinct levels of empirically observed inductive bias:

1. *Bias toward Unitary Representations:* When the target operation is a group, the learned factors naturally converge to a *unitary* representation—specifically, one unitarily equivalent to the group’s regular representation.
2. *Bias toward Group Isotopes:* In completion tasks, the model exhibits a strong inductive bias toward recovering *group isotopes*, effectively enforcing associativity.

Theoretical Challenge. Addressing these questions requires characterizing the optimization landscape of a quartic objective function \mathcal{H} subject to trilinear constraints. The complexity of this constrained optimization problem renders a direct analysis intractable.

Our Contributions. To overcome this intractability, we derive an *orthogonal decomposition* $\mathcal{H} = \mathcal{B} + \mathcal{R}$, which separates the objective into a *base term* \mathcal{B} (an inverse-scale penalty) and a *misalignment term* \mathcal{R} (enforcing directional alignment) (Section 3). This decomposition allows us to isolate the **collinear manifold** ($\mathcal{R} = 0$) as a tractable domain and derive the following results:

- *Analysis of the Manifold:* We prove that feasible collinear factorizations exist exclusively for group isotopes (Section 4). Furthermore, we show that the base term \mathcal{B} exerts a variational pressure driving factors toward unitary, full-rank representations via AM–GM equilibrium (Section 5).
- *Dominance Conjecture:* To bridge the gap to the global landscape, we formulate the *Collinearity Dominance Conjecture*. Supported by empirical evidence, we posit that the misalignment penalty \mathcal{R} acts as a dominant force over \mathcal{B} , thereby ruling out the existence of spurious non-collinear minima whenever perfect collinearity is feasible.
- *Optimality of Groups:* Conditional on this dominance, we prove that global minimizers of \mathcal{H} are necessarily unitary representations for group isotopes. Furthermore, we establish that operations not isotopic to a group incur a strictly higher objective value, theoretically formalizing the mechanism of the model’s inductive bias toward group discovery (Section 6).

- *Experimental Verification:* We provide empirical evidence supporting the Collinearity Dominance Conjecture, and demonstrate that the HyperCube objective functions as an effective differentiable proxy for algebraic associativity (Section 7).

2. Binary Operations and HyperCube Model

2.1. Binary Operations and Cayley Structure Tensors

Let (Q, \circ) denote a finite set of n elements equipped with a binary operation $\circ : Q \times Q \rightarrow Q$. Its algebraic structure is represented as an order-3 structure tensor $\delta \in \{0, 1\}^{n \times n \times n}$:

$$\delta_{abc} := \mathbb{I}_{\{a \circ b = c\}}, \quad a, b, c \in Q, \quad (1)$$

which encodes the operation table (*i.e.*, *Cayley table*). We denote $|\delta| := \sum_{a,b,c} \delta_{abc} = n^2$.

While [Huh \(2025\)](#) focused on recovering δ from partial observations (*i.e.*, completion tasks from [Power et al. \(2022\)](#)), this work analyzes the fully observed case to rigorously characterize the optimization landscape.

Groups and Quasigroups. To simplify the algebraic analysis, we restrict our scope to *quasigroups*, a subset of binary operations where the equations $a \circ x = b$ and $y \circ a = b$ possess unique solutions. Equivalently, the Cayley structure tensor δ encodes a Latin square (every slice is a permutation matrix). A *group* is then defined as a quasigroup that additionally satisfies the associativity property $(a \circ b) \circ c = a \circ (b \circ c)$.

Supported Triples. A triple (a, b, c) is called a *supported triple* if $\delta_{abc} = 1$ (*i.e.*, $a \circ b = c$). Unless otherwise noted, all indexed sums over (a, b, c) are restricted to supported triples; this is formally enforced by the factor δ_{abc} in the summand, *e.g.*, $\sum_{a,b,c} \delta_{abc}(\dots)$.

2.2. Notations

For any $X, Y \in \mathbb{C}^{n \times n}$, define the normalized Frobenius inner product and norm

$$\langle X, Y \rangle := \frac{1}{n} \text{Tr}(X^\dagger Y), \quad \|X\|^2 := \langle X, X \rangle \quad (2)$$

so that $\|U\|^2 = 1$ for any unitary U . Throughout, \dagger denotes the conjugate transpose.

2.3. HyperCube Model

Factorization. HyperCube approximates the structure tensor δ (1) via a trilinear product of parameter tensors $A, B, C \in \mathbb{C}^{n \times n \times n}$:

$$T_{abc}(\Theta) := \frac{1}{n} \text{Tr}(A_a B_b C_c), \quad \Theta := (A, B, C), \quad (3)$$

where $A_a, B_b, C_c \in \mathbb{C}^{n \times n}$ denote the matrix slices indexed by $a, b, c \in Q$. Thus, the model captures the structural three-way interactions of the indices as the product of their matrix embeddings—*i.e.*, as a *composition of linear operators*.

Objective. HyperCube minimizes a *Jacobian-based regularization* objective

$$\mathcal{H}(\Theta) := \sum_{b,c \in Q} \|B_b C_c\|^2 + \sum_{c,a \in Q} \|C_c A_a\|^2 + \sum_{a,b \in Q} \|A_a B_b\|^2, \quad (4)$$

which penalizes the squared norm of the model’s Jacobian (3) with respect to the factors (e.g., $\partial T_{abc}/\partial A_a = (B_b C_c)^\dagger$). By exploiting the Latin-square property of δ , (4) can be reformulated as a sum over supported triples, which facilitates our subsequent analysis:

$$\mathcal{H}(\Theta) = \sum_{a,b,c \in Q} \delta_{abc} (\|B_b C_c\|^2 + \|C_c A_a\|^2 + \|A_a B_b\|^2). \quad (5)$$

On the surface, this objective serves to minimize the model’s sensitivity to parameter perturbations, encouraging general robustness. However, it is not self-evident why such generic regularization induces a sharp bias toward the rigid algebraic structures of groups. Unraveling the geometric mechanism behind this surprising connection is the primary focus of our theoretical analysis.

3. Orthogonal Decomposition of \mathcal{H}

In this section, we decompose the HyperCube objective (5) into two distinct variational forces, $\mathcal{H} = \mathcal{B} + \mathcal{R}$: a **base term** \mathcal{B} (regulating factor scales) and a **misalignment term** \mathcal{R} (enforcing directional alignment).

Cauchy–Schwarz Bound The HyperCube model (3) $T_{abc} = \frac{1}{n} \text{Tr}(A_a B_b C_c)$ can be viewed as the inner product $T_{abc} = \langle A_a^\dagger, B_b C_c \rangle$. By Cauchy–Schwarz, $|T_{abc}|^2 \leq \|A_a^\dagger\|^2 \|B_b C_c\|^2 = \|A_a\|^2 \|\partial T_{abc}/\partial A_a\|^2$. Rearranging yields a lower bound on the Jacobian norm

$$\left\| \frac{\partial T_{abc}}{\partial A_a} \right\|^2 \geq \frac{|T_{abc}|^2}{\|A_a\|^2}$$

with equality if and only if A_a and $\partial T_{abc}/\partial A_a$ are *collinear*. Summing over the Jacobian terms in the objective (5) yields the following lower bound.

Lemma 1 (Base Term \mathcal{B}) *For any parameters Θ , the HyperCube objective is bounded below by*

$$\mathcal{H}(\Theta) \geq \mathcal{B}(\Theta; \delta) := \sum_{a,b,c} \delta_{abc} |T_{abc}|^2 \left(\frac{1}{\|A_a\|^2} + \frac{1}{\|B_b\|^2} + \frac{1}{\|C_c\|^2} \right) \quad (6)$$

with equality if and only if the Jacobian terms are collinear with their corresponding factor slices on every supported triple.

Definition 2 (Misalignment Matrices) *For any triple (a, b, c) , define $\Delta_{abc}^{(A)} \in \mathbb{C}^{n \times n}$ as:*

$$\Delta_{abc}^{(A)} := \frac{T_{abc}^*}{\|A_a\|^2} A_a - (B_b C_c)^\dagger \quad (7)$$

with analogous definitions for $\Delta_{abc}^{(B)}$ and $\Delta_{abc}^{(C)}$, where T_{abc}^ is the complex conjugate of T_{abc} .*

These matrices represent the component of the Jacobian orthogonal to their respective factor slices; e.g., $\langle A_a, \Delta_{abc}^{(A)} \rangle = \frac{T_{abc}^*}{\|A_a\|^2} \|A_a\|^2 - \langle A_a, (B_b C_c)^\dagger \rangle = T_{abc}^* - T_{abc}^* = 0$.

Lemma 3 (Decomposition of \mathcal{H}) *For any parameters Θ , the objective decomposes as*

$$\mathcal{H} = \mathcal{B} + \mathcal{R}, \quad \text{where} \quad \mathcal{R}(\Theta; \delta) := \sum_{a,b,c} \delta_{abc} (\|\Delta_{abc}^{(A)}\|^2 + \|\Delta_{abc}^{(B)}\|^2 + \|\Delta_{abc}^{(C)}\|^2) \geq 0. \quad (8)$$

Consequently, $\mathcal{H}(\Theta) \geq \mathcal{B}(\Theta; \delta)$ with equality if and only if $\mathcal{R}(\Theta; \delta) = 0$ (perfect collinearity).

Proof Rearrange the definition (7) to express $(B_b C_c)^\dagger = \frac{T_{abc}^*}{\|A_a\|^2} A_a - \Delta_{abc}^{(A)}$. Squaring the norm and exploiting the orthogonality $\langle A_a, \Delta_{abc}^{(A)} \rangle = 0$ yields: $\|B_b C_c\|^2 = |T_{abc}|^2 / \|A_a\|^2 + \|\Delta_{abc}^{(A)}\|^2$. Summing over the Jacobian terms in (5) yields the decomposition $\mathcal{H} = \mathcal{B} + \mathcal{R}$. ■

4. Algebraic Structure of Unitary Collinear Factorizations

The orthogonal decomposition $\mathcal{H} = \mathcal{B} + \mathcal{R}$ derived in Section 3 isolates two complementary variational forces: \mathcal{R} , which enforces perfect collinearity, and \mathcal{B} , which promotes norm maximization. Anticipating the analysis in Section 5—where we establish that \mathcal{B} drives perfectly collinear factors toward unitarity—this section analyzes the canonical solution class: *Unitary Collinear Factorizations*.

We establish a strict bidirectional correspondence between such factorizations and algebraic group structures. First, we demonstrate that groups naturally admit such factorizations via their left-regular representation. Second, we prove the converse: any unitary collinear factorization is unitarily equivalent to the regular representation, and furthermore, any quasigroup admitting such a factorization is necessarily isotopic to a group. This confirms that perfect collinearity imposes a strict structural constraint, enforcing associativity on the underlying operation.

4.1. Regular Representation Certificate for Groups

We begin by establishing the existence of unitary collinear factorizations for groups. We construct a solution using the group's left-regular representation, demonstrating that such factorizations are realizable for all group structures (and their isotopes).

Lemma 4 (Regular Representation Certificate) *Let (Q, \circ) be a finite group and let $\rho_r : Q \rightarrow U(n)$ denote its left-regular representation. The factorization defined by*

$$A_g = B_g = C_g^\dagger = \rho_r(g), \quad \forall g \in Q$$

satisfy the Cayley constraint $T(\Theta) = \delta$ and perfect collinearity $\mathcal{R}(\Theta; \delta) = 0$. Furthermore, this factorization attains the objective value:

$$\mathcal{H}(\Theta) = \mathcal{B}(\Theta; \delta) = 3|\delta|. \quad (9)$$

Proof The regular representation ρ_r is a homomorphism, meaning $\rho_r(a)\rho_r(b) = \rho_r(a \circ b)$, and its character (trace) satisfies $\text{Tr}(\rho_r(g)) = n \cdot \mathbb{I}_{\{g=e\}}$. Substituting this into (3) yields

$$T_{abc}(\Theta) = \frac{1}{n} \text{Tr}(\rho_r(a)\rho_r(b)\rho_r(c)^\dagger) = \frac{1}{n} \text{Tr}(\rho_r(a \circ b \circ c^{-1})) = \mathbb{I}_{\{a \circ b \circ c^{-1} = e\}}.$$

This expression equals 1 exactly when $a \circ b = c$ and zero otherwise, confirming $T(\Theta) = \delta$. Finally, since $\rho_r(g)$ are unitary matrices, $\|\rho_r(g)\|^2 = 1$. Summing over the $|\delta|$ supported triples in (5)–(6) yield (9). Since $\mathcal{H} = \mathcal{B} + \mathcal{R}$, we conclude $\mathcal{R}(\Theta; \delta) = 0$. \blacksquare

This result extends to group isotopes due to the equivariance of HyperCube's factorization under isotopy (Appendix B).

4.2. Uniqueness: Unitary Collinear Factorization \Rightarrow Regular Representation

Next, we address the uniqueness of this solution. We prove that any unitary collinear factorization is necessarily unitarily equivalent to the left-regular representation. We establish this result for the broader class of loops, *i.e.*, without a priori assuming associativity.

Lemma 5 (Synchronization) *Let (Q, \circ) be a finite loop (quasigroup with identity e) admitting a unitary collinear factorization $\Theta = (A, B, C)$. There exists a unitary gauge (U, V, W) , such that the gauge transformed slices $A'_g := UA_g V^\dagger, B'_g := VB_g W^\dagger, C'_g := WC_g U^\dagger$ satisfy the synchronized condition:*

$$A'_g = B'_g = (C'_g)^\dagger =: \rho(g), \quad \forall g \in Q. \quad (10)$$

Proof We construct the gauge explicitly using the identity element e . Let the gauge be $(U, V, W) = (A_e^\dagger, I_n, B_e)$. Under perfect collinearity and unitarity, the relation for the triple (g, e, g) implies $A_g B_e = C_g^\dagger$. Applying the gauge transformation:

$$A'_g = UA_g V^\dagger = A_e^\dagger A_g = A_e^\dagger (C_g^\dagger B_e^\dagger), \quad C'_g = WC_g U^\dagger = B_e C_g A_e,$$

which shows $A'_g = (C'_g)^\dagger$. Similarly, we can show $B'_g = (C'_g)^\dagger$ from the relation for (e, g, g) . Thus, all three factors collapse to a single unitary map $\rho(g)$. \blacksquare

Lemma 6 (Homomorphism and Equivalence to Regular Representation) *Let (Q, \circ) be a finite loop admitting a unitary collinear factorization. Under the synchronizing gauge of Lemma 5, the obtained map $\rho : Q \rightarrow U(n)$ satisfies the homomorphism property:*

$$\rho(a)\rho(b) = \rho(a \circ b), \quad \forall a, b \in Q.$$

Consequently, its character is identical to that of the left-regular representation ρ_r :

$$\text{Tr}(\rho(g)) = n \cdot \mathbb{I}_{\{g=e\}}, \quad \forall g \in Q.$$

This implies that ρ is injective and unitarily equivalent to ρ_r .

Proof (Homomorphism.) For any supported triple (a, b, c) , the unitary collinearity condition $A_a B_b = C_c^\dagger$ (derived from (11) with unit norms) transforms under the synchronizing gauge to $\rho(a)\rho(b) = \rho(c)$. Since $c = a \circ b$, this establishes the homomorphism property.

(Character Identity.) Evaluating the constraint on the triple (g, e, e) yields $T_{gee} = \delta_{gee}$. On the model side, we have $T_{gee} = \frac{1}{n} \text{Tr}(\rho(g)\rho(e)\rho(e)^\dagger) = \frac{1}{n} \text{Tr}(\rho(g))$. On the target side, $\delta_{gee} = \mathbb{I}_{\{goe=e\}} = \mathbb{I}_{\{g=e\}}$. Equating the two yields the character formula.

(Equivalence and Injectivity.) The derived character coincides exactly with that of the left-regular representation ρ_r . Since representations are uniquely determined by their characters, ρ is unitarily equivalent to ρ_r . Furthermore, because ρ_r is a faithful representation (injective), ρ is necessarily injective. \blacksquare

This establishes that all unitary collinear factorizations are unitarily equivalent to the canonical left-regular representation, and are therefore unitarily equivalent to each other.

4.3. Implication: Unitary Collinear Factorization \implies Associativity

Finally, building upon the uniqueness result above, we prove that the existence of a unitary collinear factorization provides a sufficient condition for group structure.

Theorem 7 (Necessity of Group Structure) *Let (Q, \circ) be a finite quasigroup admitting a unitary collinear factorization. Then, (Q, \circ) is isotopic to a group.*

Proof Every finite quasigroup (Q, \circ) is isotopic to a loop (Q, \circ') (Pflugfelder, 1990). Since the HyperCube model is equivariant under isotopy (Appendix B), the existence of a unitary collinear factorization for (Q, \circ) implies the existence of one for the loop (Q, \circ') .

Because (Q, \circ') is a loop, we can apply Lemma 5 to obtain a synchronized representation $\rho : Q \rightarrow U(n)$ satisfying the homomorphism property $\rho(x)\rho(y) = \rho(x \circ' y)$ (Lemma 6). Associativity then follows from the associativity of matrix multiplication:

$$\rho((x \circ' y) \circ' z) = \rho(x)\rho(y)\rho(z) = \rho(x \circ' (y \circ' z)).$$

Since ρ is injective (Lemma 6), this equality in representation space implies $(x \circ' y) \circ' z = x \circ' (y \circ' z)$ in the algebra. Thus, (Q, \circ') is a group, which implies (Q, \circ) is a group isotope. \blacksquare

This result confirms that the associativity imposed on the quasigroup is inherited directly from the **associativity of matrix multiplication**, fundamentally grounding the inductive bias in the model's **operator-valued factorization**.

5. Algebraic Structure under Collinearity

In this section, we analyze the algebraic consequences of perfect collinearity ($\mathcal{R} = 0$) *without* a priori assuming unitarity or the Cayley constraint $T = \delta$. The results below hold for any parameters Θ on the *collinear manifold* $\{\Theta \mid \mathcal{R}(\Theta; \delta) = 0\}$, subject only to non-degeneracy on the support (i.e., non-vanishing T_{abc} and slice norms). Our analysis establishes the variational mechanism driving the ideal structure characterized in Section 4: restricted to this manifold, the base term \mathcal{B} exerts a variational pressure that actively promotes full-rank, unitary factor slices.

Collinearity Identities. From Definition 2, *perfect collinearity* ($\mathcal{R} = 0$) reads

$$B_b C_c = \frac{T_{abc}}{\|A_a\|^2} A_a^\dagger, \quad C_c A_a = \frac{T_{abc}}{\|B_b\|^2} B_b^\dagger, \quad A_a B_b = \frac{T_{abc}}{\|C_c\|^2} C_c^\dagger, \quad (11)$$

for every supported (a, b, c) .

Lemma 8 (Shared Metric Structure) *Assume nondegeneracy and perfect collinearity $\mathcal{R}(\Theta) = 0$. Then, there exist Hermitian PSD Gram matrices $X, Y, Z \in \mathbb{C}^{n \times n}$, independent of indices, with $\text{Tr}(X) = \text{Tr}(Y) = \text{Tr}(Z) = n$, such that for every supported triple (a, b, c) :*

$$X = \frac{A_a A_a^\dagger}{\|A_a\|^2} = \frac{C_c^\dagger C_c}{\|C_c\|^2}, \quad Y = \frac{B_b B_b^\dagger}{\|B_b\|^2} = \frac{A_a^\dagger A_a}{\|A_a\|^2}, \quad Z = \frac{C_c C_c^\dagger}{\|C_c\|^2} = \frac{B_b^\dagger B_b}{\|B_b\|^2}. \quad (12)$$

Proof Fix a supported triple (a, b, c) . From the identities in (11), we have:

$$\frac{T_{abc}}{\|A_a\|^2} A_a A_a^\dagger = A_a (B_b C_c) = (A_a B_b) C_c = \frac{T_{abc}}{\|C_c\|^2} C_c^\dagger C_c.$$

Cancelling the nonzero scalar T_{abc} (nondegeneracy assumption), one obtains $A_a A_a^\dagger / \|A_a\|^2 = C_c^\dagger C_c / \|C_c\|^2$. This equality holds for all pairs (a, c) , since the Latin-square property ensures for each pair (a, c) there is a unique b on the support. Hence, the left-hand side is independent of c and the right-hand side independent of a ; denote the common matrix by X . Taking the trace yields $\text{Tr}(X) = \text{Tr}(A_a A_a^\dagger) / \|A_a\|^2 = n \|A_a\|^2 / \|A_a\|^2 = n$. The remaining equalities for Y and Z are obtained analogously. \blacksquare

Definition 9 For any supported triple, define a dimensionless scalar ratio

$$\kappa_{abc} := \frac{\|A_a\|^2 \|B_b\|^2 \|C_c\|^2}{|T_{abc}|^2}, \quad (13)$$

which is invariant under independent rescaling of factor slices: (e.g., $A_a \mapsto s_a A_a$).

Lemma 10 (κ as Normalized Rank) *Under the hypotheses of Lemma 8, κ_{abc} is constant on the support; denote the common value by κ . Then, the gram matrices satisfy $X = \kappa X^2$, $Y = \kappa Y^2$, $Z = \kappa Z^2$. Furthermore,*

$$\kappa = \frac{\text{rank}(X)}{n} \leq 1 \quad (14)$$

with equality ($\kappa = 1$) if and only if the Gram matrices are full-rank: $X = Y = Z = I_n$.

Proof Fix a supported triple (a, b, c) . Starting from $X = C_c^\dagger C_c / \|C_c\|^2$ and using the equalities in (11) and Lemma 8, one obtains

$$X = \frac{C_c^\dagger C_c}{\|C_c\|^2} = \frac{\|B_b\|^2 \|C_c\|^2}{|T_{abc}|^2} \frac{A_a (B_b B_b^\dagger) A_a^\dagger}{\|B_b\|^2} = \frac{\|B_b\|^2 \|C_c\|^2}{|T_{abc}|^2} \frac{A_a (A_a^\dagger A_a) A_a^\dagger}{\|A_a\|^2} = \kappa_{abc} X^2,$$

which yields $X = \kappa_{abc} X^2$. Since X is independent of indices, κ_{abc} must be constant (κ). Define $P := \kappa X$. Then, $P^2 = \kappa^2 X^2 = \kappa X = P$. Thus, P is an orthogonal projection, implying $\text{Tr}(P) = \text{rank}(P) = \text{rank}(X)$. Since $\text{Tr}(P) = \kappa \text{Tr}(X) = \kappa n$, we conclude $\kappa = \text{rank}(X)/n \leq 1$. If $\kappa = 1$, then $X = X^2$ with trace n , implying $X = I_n$. Analogous logic applies to Y and Z . ■

Lemma 11 (AM–GM Bound) *Under the hypotheses of Lemma 8, \mathcal{B} is bounded below by*

$$\mathcal{B}(\Theta; \delta) \geq 3\kappa^{-1/3} \sum_{a,b,c} \delta_{abc} |T_{abc}|^{4/3}, \quad (15)$$

with equality if and only if $\|A_a\|^2 = \|B_b\|^2 = \|C_c\|^2$ for every supported triple (a, b, c) .

Proof We introduce the following shorthand notation: $\alpha_a := \|A_a\|^{-2}$, $\beta_b := \|B_b\|^{-2}$, $\gamma_c := \|C_c\|^{-2}$. For each supported triple, the AM–GM inequality on the positive scalars $\alpha_a, \beta_b, \gamma_c$ yields $\alpha_a + \beta_b + \gamma_c \geq 3(\alpha_a \beta_b \gamma_c)^{1/3}$. Applying this to the definition of \mathcal{B} (6), we obtain:

$$\mathcal{B}(\Theta; \delta) := \sum_{a,b,c} \delta_{abc} |T_{abc}|^2 (\alpha_a + \beta_b + \gamma_c) \geq 3 \sum_{a,b,c} \delta_{abc} |T_{abc}|^2 (\alpha_a \beta_b \gamma_c)^{1/3}.$$

From the definition of κ (13), we have the identity $(\alpha_a \beta_b \gamma_c)^{1/3} = (\kappa |T_{abc}|^2)^{-1/3}$. Substituting this into the right-hand side, and noting that κ is constant on the support (Lemma 10), yields the claimed bound (15). Equality holds in the AM–GM step if and only if $\alpha_a = \beta_b = \gamma_c$, which is equivalent to $\|A_a\|^2 = \|B_b\|^2 = \|C_c\|^2$. ■

The above results reveal a two-stage mechanism: first, collinearity enforces a rigid, shared metric structure (i.e., constant Gram matrices) across all factor slices (Lemma 8). Within this framework, Lemma 10 identifies κ as the shared normalized rank. Consequently, since minimizing \mathcal{B} maximizes κ (Lemma 11), the base term exerts a variational pressure that drives these rigid Gram matrices to their full-rank limit, enforcing unitarity. This demonstrates a **harmonious collaboration**: the misalignment term drives collinearity, while the base term promotes rank expansion.

6. Optimality under Collinearity Dominance

We now formally address the global constrained optimization problem over the feasible set $\mathcal{F}_\delta := \{\Theta \mid T(\Theta) = \delta\}$:

$$\mathcal{H}_{\min}(\delta) := \min_{\Theta \in \mathcal{F}_\delta} \mathcal{H}(\Theta), \quad (16)$$

which defines the *minimum objective value* for the given task δ . By analyzing this global landscape, we aim to resolve the two fundamental challenges posed in Section 1. Specifically, we seek to characterize the optimal parameters Θ^* for given tasks (explaining the *Unitary Collinearity Bias*) and compare the minimum objective values $\mathcal{H}_{\min}(\delta)$ across different algebraic structures (explaining the *Group Isotope Bias*).

Analytical Strategy. Direct analysis of (16) is intractable due to the complex geometry of the trilinear feasible set. To overcome this, we adopt a two-stage strategy. First, we rely on the analysis of the *collinear manifold* from Sections 4–5, where the problem is tractable and yields rigid algebraic structures. Second, to extend these insights to the global landscape, we introduce conjectures that relax the collinearity constraint, positing the dominance of the misalignment penalty \mathcal{R} over \mathcal{B} —a hypothesis grounded in the robust empirical observations.

Theorem 12 (Optimality of Unitary Structure) *Let (Q, \circ) be a finite quasigroup that admits a feasible collinear factorization (i.e., a group isotope). Restricted to the feasible collinear manifold $\mathcal{F}_\delta \cap \{\Theta \mid \mathcal{R}(\Theta; \delta) = 0\}$, the minimum of \mathcal{H} is achieved by a **unitary** collinear factorization (unique up to gauge symmetry), attaining the value $\mathcal{H}_{\min}(\delta) = 3|\delta|$.*

Proof Within the collinear manifold, the optimization problem reduces to attaining the AM–GM bound in Lemma 11, which reduces to $\mathcal{B}(\Theta) \geq 3\kappa^{-1/3}|\delta|$ under the constraint $T = \delta$. Since the lower bound is a strictly decreasing function of the rank coefficient κ , it is uniquely minimized at the maximum rank $\kappa = 1$. To achieve the bound $\mathcal{B} = 3|\delta|$, the AM–GM equality condition must hold. For $\kappa = 1$ and $|T_{abc}| = 1$, this necessitates $\|A_a\|^2 = \|B_b\|^2 = \|C_c\|^2 = 1$ for all supported triples. Since the support graph of a quasigroup is connected, this enforces unitarity across all slices. Thus, the minimizer is a unitary collinear factorization. ■

This theorem confirms that restricted to the collinear manifold, minimizing the base term \mathcal{B} strictly enforces unitarity. Consequently, the structurally optimal solution on the manifold is necessarily a unitary collinear factorization.

Remark 13 *In addition to the base term’s variational pressure, the Cayley constraint $T = \delta$ independently enforces full rank within the collinear manifold (Lemma 21, Appendix C). Crucially, however, the variational pressure applies even when the constraint is relaxed (e.g., in noisy or partially observed settings).*

6.1. The Landscape Gap: Spurious Minima

While the preceding analysis establishes that unitary collinear factorizations are optimal *within* the manifold ($\mathcal{R} = 0$), it offers no guarantees for the landscape behavior outside it ($\mathcal{R} > 0$). This leaves open the theoretical possibility of *spurious minima*—non-collinear local basins that could trap optimization, even when a perfectly collinear factorization is feasible.

Empirical observation, however, strongly argues against such spurious minima. For group isotopes, optimization consistently converges to the collinear manifold from random initializations. This implies that the variational pressure from the base term \mathcal{B} is insufficient to prevent collinearity, suggesting that the misalignment penalty acts as a **globally dominant force** in the landscape.

In the following subsections, we formalize this intuition via conjectures, positing that the misalignment penalty \mathcal{R} dominates the landscape.

6.2. The Collinearity Dominance Conjecture

We formalize the empirical intuition established in Section 6.1 via the following conjectures. The first posits that the optimization landscape prioritizes perfect collinearity over the reduction of the base term, ensuring that solutions do not drift off the collinear manifold when a feasible point exists.

Conjecture 14 (Weak Collinearity Dominance) *Let δ be a target operation that admits a feasible collinear factorization (i.e., the set $\{\Theta \in \mathcal{F}_\delta \mid \mathcal{R}(\Theta; \delta) = 0\}$ is non-empty). Then, every global minimizer of the constrained problem (16) lies on the collinear manifold $\mathcal{R} = 0$.*

Conditional on this conjecture, we can extend the local analysis of Theorem 12 to the global landscape. This confirms that for group tasks, the global optimum is not just collinear, but specifically the unitary regular representation.

Theorem 15 (Global Optimality for Group Isotopes) *Let δ be the Cayley tensor of a finite quasigroup that admits a feasible collinear factorization (i.e., a group isotope). Then, under Conjecture 14, every global minimizer of the constrained problem (16) is a **unitary** collinear factorization, achieving the minimum value $\mathcal{H}_{\min}(\delta) = 3|\delta|$.*

Proof This follows directly from Theorem 12 and Conjecture 14. By the conjecture, any global minimizer must satisfy $\mathcal{R} = 0$. Consequently, the problem reduces to minimizing \mathcal{B} on the collinear manifold. By Theorem 12, this minimum is attained exclusively by unitary factorizations. \blacksquare

6.3. Strong Dominance and Variational Trade-off

Motivation. The Weak Conjecture ensures the stability of the collinear manifold for group isotopes. However, for **non-group isotopes**, the collinear manifold is empty ($\mathcal{R} > 0$), making collinear alignment impossible. In this setting, the objectives \mathcal{B} and \mathcal{R} could enter a direct variational trade-off, potentially sacrificing collinearity to further reduce the base term.

To characterize the inductive bias in this general setting, we propose that the landscape is governed by a strict **variational hierarchy**: specifically, that the penalty imposed by misalignment always outweighs potential reductions in the base term.

Conjecture 16 (Strong Collinearity Dominance) *Let (Q, \circ) be a finite quasigroup. For any feasible factorization $\Theta \in \mathcal{F}_\delta$, we posit that the misalignment penalty \mathcal{R} strictly dominates the variational trade-off: any reduction in the base term \mathcal{B} achieved by **sacrificing collinearity** is strictly outweighed by the resulting increase in \mathcal{R} .*

A sufficient (though not necessary) quantitative condition capturing this dominance is the existence of a constant $c \in [0, 1]$ such that:

$$\mathcal{B}(\Theta; \delta) \geq 3|\delta| - c\mathcal{R}(\Theta; \delta). \quad (17)$$

Under this linear condition, the HyperCube objective satisfies

$$\mathcal{H} \geq 3|\delta| + (1 - c)\mathcal{R}. \quad (18)$$

Since $c < 1$, any misaligned solution ($\mathcal{R} > 0$) strictly increases the total cost, implying Conjecture 14.

6.4. Bias towards Group Isotopes

Finally, we characterize which binary operations minimize $\mathcal{H}_{\min}(\delta)$. This establishes the inductive bias of the model against non-associative structures.

Proposition 17 (Coercivity of Misalignment) *Let δ be the Cayley tensor of a finite quasigroup. If δ is **not** isotopic to a group, then the misalignment term is bounded away from zero on the feasible set:*

$$\inf_{\Theta \in \mathcal{F}_{\delta}} \mathcal{R}(\Theta; \delta) =: \rho_{\min} > 0. \quad (19)$$

Proof We proceed by contradiction. Suppose $\inf \mathcal{R} = 0$. Then there exists a sequence $\{\Theta^{(k)}\} \subset \mathcal{F}_{\delta}$ such that $\mathcal{R}(\Theta^{(k)}) \rightarrow 0$. Consider the sublevel set $S_M = \{\Theta \in \mathcal{F}_{\delta} \mid \mathcal{H}(\Theta) \leq M\}$ containing this sequence.

Recall that $\mathcal{H} \geq \mathcal{B}$. Since \mathcal{B} is a sum of inverse squared norms, factor norms in S_M are bounded away from zero. Because factors cannot vanish, the product terms in \mathcal{H} prevents any norm from diverging to infinity (as divergence would require a vanishing partner to keep the product finite). Thus, S_M is compact (modulo unitary gauge), ensuring the sequence accumulates to a limit point Θ^* with $\mathcal{R}(\Theta^*) = 0$. By Theorem 7, this implies δ is isotopic to a group, contradicting the hypothesis. \blacksquare

Theorem 18 (Strict Gap for Non-Groups) *Assume Conjecture 16 holds. The minimum HyperCube objective satisfies:*

$$\mathcal{H}_{\min}(\delta) \geq 3|\delta|, \quad (20)$$

with equality if and only if δ is isotopic to a group. Consequently, among all quasigroups of fixed order n , group isotopes achieve the strictly minimal objective value \mathcal{H}_{\min} .

Proof (\Leftarrow) If δ is a group isotope, Lemma 4 (via isotopy equivariance) guarantees the existence of a solution with $\mathcal{H} = 3|\delta|$.

(\Rightarrow) Suppose δ is not a group isotope. By Proposition 17, $\inf_{\mathcal{F}_{\delta}} \mathcal{R} = \rho_{\min} > 0$. Applying the dominance inequality (17): $\mathcal{H}_{\min}(\delta) \geq 3|\delta| + (1 - c)\rho_{\min}$. Since $c < 1$ and $\rho_{\min} > 0$, the gap is strictly positive. This establishes the inductive bias: HyperCube assigns strictly higher cost to non-associative operations (up to isotopy). \blacksquare

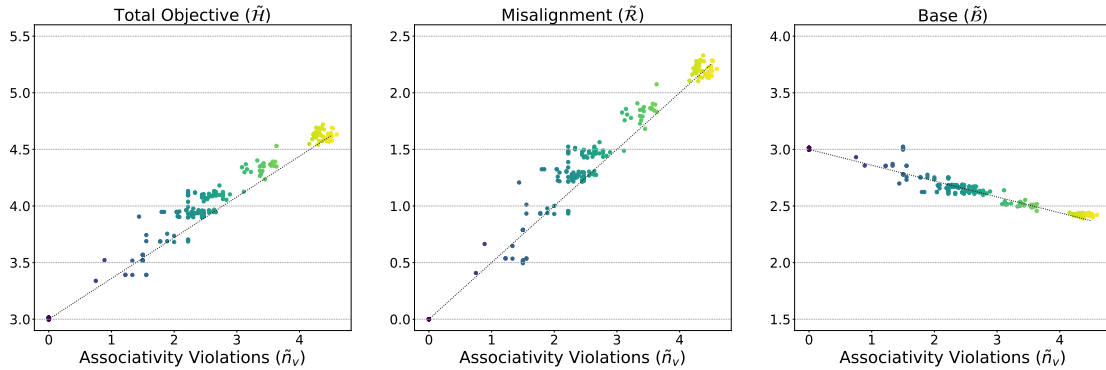


Figure 1: Empirical verification of Strong Collinearity Dominance. Scatter plots showing the normalized objective terms ($\tilde{\mathcal{H}}, \tilde{\mathcal{R}}, \tilde{\mathcal{B}}$) versus the normalized associativity violation \tilde{n}_v for Latin squares corresponding to loops of orders $n \in \{5, 6, 7, 8\}$. (Middle) The misalignment penalty $\tilde{\mathcal{R}}$ grows linearly with non-associativity ($c_R \approx 0.50$). (Right) The base term $\tilde{\mathcal{B}}$ decreases linearly ($c_B \approx 0.14$), confirming variational trade-off. (Left) The total objective $\tilde{\mathcal{H}}$ exhibits a net positive slope ($c_H \approx 0.36$), confirming that the misalignment penalty dominates the trade-off, forcing the global minimum to the group structure ($\tilde{n}_v = 0$).

7. Empirical Verification: Associativity and Dominance

Objective. We empirically investigate the **Strong Collinearity Dominance Conjecture** (Conjecture 16). Specifically, we aim to quantify the variational trade-off between the misalignment penalty \mathcal{R} and the base term \mathcal{B} . Recall that the conjecture posits a bound $\mathcal{B} \geq 3|\delta| - c\mathcal{R}$ with $c < 1$, implying that the savings in \mathcal{B} are outweighed by the penalty in \mathcal{R} .

Experimental Setup. We analyze Latin squares δ corresponding to loops of orders $n \in \{5, 6, 7, 8\}$. For the smaller orders $n \in \{5, 6\}$, we exhaustively evaluate all unique loops up to isomorphism (6 and 106 cases, respectively). For $n \in \{7, 8\}$, we evaluate a random subset of 100 loops per order, due to the combinatorial explosion of the search space (e.g., 23,746 unique loops for $n = 7$). For each δ , we compute the global minimum $\mathcal{H}_{\min}(\delta)$ using a gradient-based optimizer with multiple random initial values to mitigate local minima. To correlate the landscape geometry with algebraic structure, we measure the normalized associativity violations:

$$\tilde{n}_v(\delta) := \frac{1}{|\delta|} \sum_{a,b,c} \mathbb{I}_{\{(a \circ b) \circ c \neq a \circ (b \circ c)\}}.$$

Note that $\tilde{n}_v = 0$ if and only if δ encodes a group.

Results. We analyze the normalized objective terms ($\tilde{\mathcal{R}} := \mathcal{R}_{\min}/|\delta|$, $\tilde{\mathcal{B}} := \mathcal{B}_{\min}/|\delta|$, $\tilde{\mathcal{H}} := \mathcal{H}_{\min}/|\delta|$) as a function of the violation metric \tilde{n}_v . The data reveals a striking linear

scaling law across the space of Latin squares:

$$\begin{aligned}\tilde{\mathcal{R}}(\delta) &\approx c_R \cdot \tilde{n}_v(\delta) & (c_R \approx 0.50) \\ \tilde{\mathcal{B}}(\delta) &\approx 3 - c_B \cdot \tilde{n}_v(\delta) & (c_B \approx 0.14) \\ \tilde{\mathcal{H}}(\delta) &\approx 3 + c_H \cdot \tilde{n}_v(\delta) & (c_H = c_R - c_B \approx 0.36).\end{aligned}\tag{21}$$

Confirmation of Dominance. These scaling laws provide precise quantitative verification of the *Strong Collinearity Dominance Conjecture* (Conjecture 16). We identify the constant c in the conjectured bound $\mathcal{B} \geq 3|\delta| - c\mathcal{R}$ as the ratio of the empirical slopes:

$$c \approx \frac{c_B}{c_R} \approx \frac{0.14}{0.50} = 0.28.$$

Since $c \approx 0.28 < 1$, the variational “savings” in the base term \mathcal{B} are strictly dominated by the misalignment penalty \mathcal{R} , effectively confining the optimization trajectory to the collinear manifold.

A Differentiable Proxy for Group Isotopy. This net positive coefficient ($c_H > 0$) confirms that the global minima of \mathcal{H} are strictly confined to the set of group isotopes ($\tilde{n}_v = 0$). This establishes \mathcal{H}_{\min} as a **differentiable proxy for group structure**.

Crucially, \mathcal{H}_{\min} is an **isotopy invariant** quantity. Detecting such intrinsic algebraic properties usually requires solving combinatorial graph isomorphism problems; remarkably, HyperCube achieves this via continuous optimization, successfully abstracting away arbitrary relabeling to detect the underlying **latent group structure** encoded in the data.

Remark: Breaking Isotopy Symmetry. While \mathcal{H} is invariant under the full isotopy group ($S_n \times S_n \times S_n$), practical applications often require recovering the canonical group operation (e.g., to derive equivariant layers). As shown in Huh (2025), this ambiguity can be resolved by enforcing the parameter tying constraint $A_g = B_g = C_g^\dagger, \forall g \in Q$. This constraint breaks the isotopy symmetry down to isomorphism symmetry, forcing the model to align the identity element and recover the specific group table structure.

8. Conclusion and Future Work

Our analysis provides the first rigorous theoretical framework explaining the HyperCube model’s strong inductive bias toward discovering groups and their unitary representations. By deriving the orthogonal decomposition $\mathcal{H} = \mathcal{B} + \mathcal{R}$, we identified the collinear manifold ($\mathcal{R} = 0$) as the central tractable domain where the optimization landscape simplifies to rigid algebraic constraints.

Within this manifold, we established that the misalignment penalty \mathcal{R} acts as a structural filter enforcing associativity, while the base term \mathcal{B} exerts a variational pressure that drives the representation to its full-rank, unitary limit. Crucially, our investigation of the global landscape suggests a strict variational hierarchy: theoretical arguments and empirical results confirm that the cost of misalignment strictly outweighs the potential savings from norm inflation. This dominance ensures that the global minimum is exclusively reserved for group isotopes, effectively confining the final solution to the collinear manifold where the full-rank and unitary biases are mathematically guaranteed.

This analysis highlights a distinctive property of HyperCube: a systematic bias toward full-rank, unitary representations. This stands in sharp contrast to the prevalent “low-rank simplicity bias” observed in standard deep learning models (Arora et al., 2019; Jacot, 2023; Huh et al., 2023; Balzano et al., 2025). Thus, HyperCube’s unitarity bias suggests a novel class of neural inductive biases better suited for discovering discrete algebraic structures, moving beyond the limits of interpolation-based generalization.

Open Analytical Challenges. The central open challenge remains the analytic proof of the *Strong Collinearity Dominance Conjecture* to close the theoretical gap for non-group isotopes. Additionally, while we proved the rank-maximizing pressure of \mathcal{B} within the collinear manifold, characterizing its spectral behavior in the highly misaligned regime remains an open analytical question. Extending these dominance arguments to the partial observation regime would theoretically ground the model’s performance in tensor completion tasks.

Future Directions. We aim to generalize this algebraic structure discovery mechanism to neural architectures operating on raw data, developing deep learning models with an inherent bias toward discovering generalizable high-level principles. In this framework, the symmetry group represents the *invariant causal laws* underlying the data, rather than a mere statistical artifact. Discovering this structure enables the model to distinguish true universal laws from spurious statistical correlations, offering a principled path to address fundamental limitations of current AI systems—including sample inefficiency, hallucinations, and the lack of systematic OOD (out-of-domain) generalization.

References

Sanjeev Arora, Nadav Cohen, Wei Hu, and Yuping Luo. Implicit Regularization in Deep Matrix Factorization, October 2019. URL <http://arxiv.org/abs/1905.13655>. arXiv:1905.13655 [cs, stat].

Laura Balzano, Tianjiao Ding, Benjamin D Haefele, Soo Min Kwon, Qing Qu, Peng Wang, Zhangyang Wang, and Can Yaras. An overview of low-rank structures in the training and adaptation of large models. *arXiv preprint arXiv:2503.19859*, 2025.

Michael M. Bronstein, Joan Bruna, Taco Cohen, and Petar Veličković. Geometric Deep Learning: Grids, Groups, Graphs, Geodesics, and Gauges, May 2021. URL <http://arxiv.org/abs/2104.13478>. arXiv:2104.13478 [cs, stat].

Taco Cohen and Max Welling. Group Equivariant Convolutional Networks. In *Proceedings of The 33rd International Conference on Machine Learning*, pages 2990–2999. PMLR, June 2016. URL <https://proceedings.mlr.press/v48/cohenc16.html>. ISSN: 1938-7228.

Robert Geirhos, Jörn-Henrik Jacobsen, Claudio Michaelis, Richard Zemel, Wieland Brendel, Matthias Bethge, and Felix A Wichmann. Shortcut learning in deep neural networks. *Nature Machine Intelligence*, 2(11):665–673, 2020.

David J Gross. The role of symmetry in fundamental physics. *Proceedings of the National Academy of Sciences*, 93(25):14256–14259, 1996.

Dongsung Huh. Discovering group structures via unitary representation learning. In *The Thirteenth International Conference on Learning Representations*, 2025. URL <https://openreview.net/forum?id=Tz8Li6G2xU¬eId=Tz8Li6G2xU>.

Minyoung Huh, Hossein Mobahi, Richard Zhang, Brian Cheung, Pulkit Agrawal, and Phillip Isola. The Low-Rank Simplicity Bias in Deep Networks, March 2023. URL <http://arxiv.org/abs/2103.10427>. arXiv:2103.10427 [cs].

Arthur Jacot. Implicit Bias of Large Depth Networks: a Notion of Rank for Nonlinear Functions, March 2023. URL <http://arxiv.org/abs/2209.15055>. arXiv:2209.15055 [cs, stat].

Ziwei Ji, Nayeon Lee, Rita Frieske, Tiezheng Yu, Dan Su, Yan Xu, Etsuko Ishii, Ye Jin Bang, Andrea Madotto, and Pascale Fung. Survey of hallucination in natural language generation. *ACM computing surveys*, 55(12):1–38, 2023.

Brenden Lake and Marco Baroni. Generalization without systematicity: On the compositional skills of sequence-to-sequence recurrent networks. In *International conference on machine learning*, pages 2873–2882. PMLR, 2018.

Emmy Noether. Invariante variationsprobleme. In *Gesammelte Abhandlungen-Collected Papers*, pages 231–239. Springer, 1918.

Hala O Pflugfelder. *Quasigroups and Loops: Introduction*, volume 7 of *Sigma Series in Pure Mathematics*. Heldermann Verlag, Berlin, 1990.

Alethea Power, Yuri Burda, Harri Edwards, Igor Babuschkin, and Vedant Misra. Grokking: Generalization Beyond Overfitting on Small Algorithmic Datasets, January 2022.

Ashish Vaswani, Noam Shazeer, Niki Parmar, Jakob Uszkoreit, Llion Jones, Aidan N Gomez, Łukasz Kaiser, and Illia Polosukhin. Attention is all you need. *Advances in neural information processing systems*, 30, 2017.

Eugene Paul Wigner. *Symmetries and Reflections. Scientific Essays of Eugene P. Wigner*. Indiana University Press, 1967.

Appendix A. Enumeration and Symmetry Classes

While the main text formulates the problem for general quasigroups, our experimental analysis (Section 7) relies on the enumeration of loops to track the search space size.

Loops and Reduced Latin Squares. A loop is a quasigroup with a two-sided identity element $e \in Q$. If we label the elements of Q as $\{0, 1, \dots, n-1\}$ with $0 = e$, the operation table is a *reduced* (or normalized) Latin square, where the first row and first column are in natural order $(0, 1, \dots, n-1)$. Classifying loops of order n is equivalent to classifying reduced Latin squares of order n .

Isomorphism vs. Isotopy. The enumeration of distinct structures depends on the chosen notion of equivalence:

- **Loop Isomorphism (Simultaneous Relabeling):** Two loops are isomorphic if they differ by a bijection $\phi : Q \rightarrow Q'$ satisfying $\phi(a) \circ' \phi(b) = \phi(a \circ b)$. In terms of Latin squares, this corresponds to applying the *same* permutation to rows, columns, and symbol labels simultaneously. We use this relation to identify unique loops.
- **Quasigroup Isotopy (Independent Relabeling):** The HyperCube model, which treats the operation as a 3-way tensor without a privileged identity, naturally respects a larger internal symmetry group. Two Latin squares are *isotopic* if they differ by an arbitrary triple of permutations $(\phi, \psi, \chi) \in S_n \times S_n \times S_n$ acting independently on rows, columns, and symbols.

Since the HyperCube objective is invariant under this larger group (see Appendix B), counting distinct structures for the model corresponds to counting quasigroup isotopy classes (orbits of S_n^3).

Appendix B. Symmetry Properties of HyperCube

This section details the equivariance and invariance properties of the HyperCube product and objective.

B.1. Isotopy Equivariance

Let $\Theta' = (A', B', C')$ be the parameters obtained by permuting indices according to bijections (ϕ, ψ, χ) : $A'_a := A_{\phi(a)}$, $B'_b := B_{\psi(b)}$, $C'_c := C_{\chi(c)}$.

Lemma 19 (Isotopy Equivariance) *For any index permutation triple, $T_{abc}(\Theta') = T_{\phi(a)\psi(b)\chi(c)}(\Theta)$.*

Proof Follows immediately from direct index substitution into the trace definition $T_{abc} = \frac{1}{n} \text{Tr}(A_a B_b C_c)$. Consequently, if Θ factorizes a tensor δ , then Θ' factorizes the isotopic tensor δ' . \blacksquare

B.2. Gauge Invariance

Let (U, V, W) be unitary matrices. Define the gauge-transformed slices: $A'_a := UA_aV^\dagger$, $B'_b := VB_bW^\dagger$, $C'_c := WC_cU^\dagger$.

Lemma 20 (Gauge Invariance) *The HyperCube product tensor $T(\Theta)$ and objective $\mathcal{H}(\Theta)$ are invariant under unitary gauge transformations.*

Proof *Product Tensor:* Using the cyclicity of the trace,

$$T'_{abc} = \frac{1}{n} \text{Tr}(UA_aV^\dagger VB_bW^\dagger WC_cU^\dagger) = \frac{1}{n} \text{Tr}(A_aB_bC_cU^\dagger U) = T_{abc}.$$

Objective: The Frobenius norm is unitary invariant. For any term in \mathcal{H} , e.g., $\|B'_bC'_c\|^2$, the internal unitary factors cancel ($W^\dagger W = I$) and the external factors (V, U^\dagger) disappear under the norm $\|X\|^2 = \text{Tr}(X^\dagger X)$. Thus $\mathcal{H}(\Theta') = \mathcal{H}(\Theta)$. ■

This invariance allows us to apply the *synchronizing gauge* used in Lemma 5 without loss of generality.

Appendix C. Full-rank Structure under Cayley Constraint

We show that satisfying the exact Cayley constraint $T(\Theta) = \delta$ enforces full rank on the collinear manifold, independent of the base term \mathcal{B} .

Lemma 21 (Structural Full-Rank under Cayley Constraint) *Let δ be the Cayley tensor of a quasigroup of order n . If Θ is a feasible factorization ($T(\Theta) = \delta$) that satisfies perfect collinearity ($\mathcal{R}(\Theta; \delta) = 0$), then the common Gram matrix X has full rank (n). Consequently, $\kappa = 1$.*

Proof We analyze the rank of the mode-1 unfolding $T_{(1)} \in \mathbb{C}^{n \times n^2}$, where rows correspond to index a and columns to indices (b, c) .

1. Rank of the Target (δ). Since δ encodes a Latin square, for any fixed c , the slice $\delta_{::c}$ is a permutation matrix. Consequently, the columns of the unfolding $\delta_{(1)}$ span the entire ambient space \mathbb{C}^n . The feasibility constraint $T(\Theta) = \delta$ therefore requires:

$$\text{rank}(T_{(1)}) = n.$$

2. Range of the Model. We bound the range of the model's unfolding to show it is limited by X .

- *Collinearity Constraint:* Under perfect collinearity ($\mathcal{R} = 0$), Lemma 8 implies $A_a A_a^\dagger = \alpha_a^2 X$. Thus, the image of every slice A_a lies within the image of X :

$$\text{Range}(A_a) \subseteq \text{Range}(X), \quad \forall a \in Q.$$

- *Trace Linearity:* The model defines entries as $T_{abc} = \frac{1}{n} \text{Tr}(A_a(B_bC_c))$. Viewing $T_{(1)}$ as a linear map from inputs (b, c) to outputs a , its image lies within the span of the ranges of the factor matrices $\{A_a\}$.

Combining these, the column space of the unfolded model is constrained by X :

$$\mathbb{C}^n = \text{Range}(T_{(1)}) \subseteq \text{Span} \left(\bigcup_a \text{Range}(A_a) \right) \subseteq \text{Range}(X).$$

Since $X \in \mathbb{C}^{n \times n}$, the containment $\mathbb{C}^n \subseteq \text{Range}(X)$ implies X has full rank n . \blacksquare

Remark 22 *This result complements Theorem 12. While Theorem 12 shows that \mathcal{B} exerts a variational pressure toward full rank (important for partial observations), Lemma 21 shows that the constraint $T = \delta$ independently enforces full rank within the collinear manifold.*